INTERNATIONAL ATOMIC ENERGY AGENCY
UNITED NATIONS EDUCATIONAL, SCIENTIFIC AND CULTURAL ORGANIZATION

INTERNATIONAL CENTRE FOR THEORETICAL PHYSICS
34100 TRIESTE (ITALY) - P.O.B. 586 - MIRAMARE - STRADA COSTIERA 11 - TELEPHONES: 224281/2/3/4/5/6
CABLE: CENTRATOM - TELEX 460392-1

SMR/100 - 20

WINTER COLLEGE ON LASERS, ATOMIC AND MOLECULAR PHYSICS

(24 January - 25 March 1983)

Laser Double-Resonance Spectroscopy in Molecular Physics

W. DEMTRÖDER

Fachbereich Physik
Universität Kaiserslautern
Postfach 3049
6750 Kaiserslautern
Fed. Rep. Germany

[illegible]

[illegible] PHYSICS

[illegible]

SMR\100 - 20

[illegible] MOLECULAR PHYSICS

[illegible] 1982)

[illegible] Spectroscopy in Molecular Physics

[illegible]

[illegible] Kaiserslautern

[illegible] Atmosphere Physik

[illegible] Kaiserslautern

[illegible]

Fed. Rep. Germany

[illegible] only for distribution to participants.

[illegible] from [illegible] 20.

Laser Double-Resonance Spectroscopy in Molecular Physics

W. Demtröder

Fachbereich Physik, Universität Kaiserslautern

I. Introduction

Detailed experimental investigations of electronic transitions in diatomic or polyatomic molecules and closer examinations of excited molecular states are often impeded by fundamental difficulties: The visible and ultraviolet spectra of many molecules show an exceedingly high spectral line density where many lines overlap within their Doppler-width. The application of "classical", Doppler-limited spectroscopic techniques to such cases often yields quasicontinuous spectra concealing many finer details such as rotational structure or fine- and hyperfine splittings. Furthermore, the excited states of molecules often have a perturbed level structure which results in congested and irregular spectra and makes their assignment a tedious task.

On the other hand a more thorough knowledge of excited molecular states is highly desirable since they play an important role in chemical reactions. All light-induced reactions, as for example photobiological processes, proceed via electronically excited states. Although studies of laser induced chemical reactions have gained increasing interest, our knowledge of the detailed structure of excited states is still insufficient.

There are several ways to overcome the experimental difficulties. Either the spectral resolution can be increased beyond the limit of the Doppler-width, or the number of lines has to be reduced. The first solution is based on Doppler-free spectroscopic techniques such as saturation spectroscopy [1], polarization spectroscopy [2] or linear laser spectroscopy in collimated molecular beams [3]. The reduction of the number of thermally populated absorbing levels and thus of the density of lines may be achieved by a drastic decrease of the temperature, down to a few Kelvin. Molecular spectroscopy at such low temperatures can be realized for instance in supersonic molecular beams where adiabatic cooling during the expansion from a high pressure region into the vacuum results in rotational temperatures down to below 1 K [4].

Laser double resonance spectroscopy is capable of combining both advantages for the investigation of complex molecular spectra: They allow Doppler-free resolution and they reduce the number of detected molecular transitions to those few which start from a single selected level. Many different double resonance schemes have been applied so far to molecular spectroscopy, using either two lasers or one laser and a microwave or radiofrequency field.

Figure 1 illustrates schematically three possible schemes of optical-optical double resonance (OODR) where two independent lasers are utilized: a pump laser which is stabilized on a selected transition between two levels i and k and a tunable probe laser which is scanned through the spectral range of interest and monitors all those transitions connected either with level i or with level k. The beams from the two lasers may travel collinear or antiparallel through the sample.

The pump laser "labels" both levels i and k either by changing their popula-

tions N_i, N_k due to optical pumping or by altering the orientation of molecules in these levels. Both effects will change the absorption or induced emission of the probe laser or its state of polarization which can be monitored with appropriate detection techniques.

Pulsed lasers as well as cw lasers can be used. Both types have their advantages and disadvantages as will be discussed below. In case of cw lasers it is convenient to chop the pump intensity at a frequency f with a period 1/f long compared to the relaxation time of the pumped level. This guarantees quasi-stationary conditions during the pump cycle. The populations N_i and N_k are then switched at the frequency f between the thermal populations $N_i^{(0)}$, $N_k^{(0)}$ with the pump laser off and the values $N_i^{(L)}$, $N_k^{(L)}$ with the pump laser on. When the probe laser absorption is monitored at the frequency f with phase sensitive detection techniques, only those transitions are detected which are connected either with level i or with level k.

We will now discuss the three schemes of Fig. 1 in more detail and illustrate them by several examples.

II. Optical-optical double resonance with a common lower level

The double resonance scheme of Fig. 1a may be regarded as an inversion of laser induced fluorescence (see Fig. 2). The LIF method is based on the selective population of a vibrational rotational level $(v'_k\ J'_k)$ in an excited electronic state. The fluorescence spectrum, emitted from this level is simple and readily assigned. It gives information about the levels $m=(v'',J'')$ of the lower state on which the fluorescence terminates. The double resonance signals, on the other hand, consist of all allowed transitions from the lower level (v''_i, J''_i), labelled by the pump laser, to all accessible levels (v'_m, J'_m) of upper electronic states. The upper levels k and m of pump and probe transitions may belong to the same electronic state or to different states.

The method is of particular advantage when the upper state reached by the probe laser is perturbed. In this case many lines will be shifted from their regular position and it is by no means trivial to assign such lines in a normal absorption spectrum, even if all lines are resolved. The double resonance signals, however, are much easier to identify since the lower level (v''_i, J''_i) of each probe transition is already known from the pump transition. The selection rules for optically allowed transitions leave only a few choices for upper levels (v'_m, J'_m).

In diatomic molecules, for example, the selection rule $\Delta J = \pm 1,0$ for the rotational quantum number J allows only rotational levels with $J'_m = J''_i \pm 1$ or $J'_m = J''_i$ to be reached by the probe laser.[5] If the lower electronic state i and the upper state m both are Σ-states, only transitions with $\Delta J = \pm 1$ are allowed and the spacings of the two double resonance signals to levels $(v', J''_i + 1)$ and $(v', J''_i - 1)$ immediately yield the rotational spacings in the upper state.

When pulsed lasers with larger bandwidth than that of single mode cw lasers are applied to double resonance spectroscopy of complex spectra, several molecular transitions may fall within the bandwidth of the pump laser, which therefore simultaneously labels several levels i_1, i_2 ... . The probe laser then monitors all accessible transitions from these levels and the double resonance spectrum may loose some of its simplicity. Even when single mode cw lasers are used in

gas or vapor cells with Doppler-broadened absorption lines, all transitions which overlap with the pump laser wavelength within the Doppler-width can be pumped and give rise to double resonance signals. The intensities of the double resonance signals depend on the change $\Delta N = N_i^{(0)} - N_i^{(L)}$ induced by the pump laser. Those transitions which overlap only on the far wings of their Doppler profiles with the pump laserwavelength will be therefore less intense than the selected transition which coincides exactly with the pump laser.

There are two further effects which increase the number of possible double-resonance signals. These are due to fluorescence from the pumped upper level k and to collisional energy transfer between the pumped lower level i and neighbouring levels (v", J") (Fig. 3). The fluorescence from level (v_k', J_k') populates many lower levels (v", J") (see Fig. 2b), according to the Franck-Condon factors of the fluorescence transitions ($v_k' \rightarrow v"$). Because the spontaneous lifetime of the upper level is generally much shorter than the chopping period 1/f, the phase of the population modulation, caused by the chopped pump laser, is for these levels (v", J") the same as for level k, but opposite to that of level i.

Since the pump laser depletes the population N_i of level i below the thermal equilibrium value $N_i^{(0)}$, collision induced transitions from neighbouring levels to i will occur more frequently than collisions which depopulate level i. This means that the populations N(v",J") of these adjacent levels will also decrease during the period where the pump laser is on. The population decrease ΔN_j of a level ($v_j"$, $J_j"$) depends on the population change $\Delta N_i = N_i^{(0)} - N_i^S$, on the collision cross section σ_{ij} and the density of colliding molecules. Measurements of the ratios $\Delta N_j/\Delta N_i$ can be used to determine these cross sections (see below).

For high resolution spectroscopy of dense spectra all these effects may impede the assignment of the double resonance signals. They can be eliminated by combining the OODR-method with Doppler-free techniques under collision free conditions. Two examples shall illustrate this.

The first example demonstrates the application of OODR spectroscopy to the assignment of lines in the extremely complex visible spectrum of NO_2. The experimental arrangement is shown in Fig. 4. The beams from two single mode lasers cross the collimated molecular beams perpendicularly. Both beams pass through a chopper wheel with two different rows of holes. The pump beam intensity I_1 is chopped at a frequency f_1, the probe beam intensity I_2 at a frequency f_2. The fluorescence induced by both lasers is used to monitor the absorption. The population density N_i of molecules, having passed through the pump beam, is

$$N_i^{(L)} = N_i^0(1 - a \cdot I_1) \tag{1}$$

The fluorescence intensity induced by the probe laser, which crosses the molecular beam a few mm downstreams from the pump laser is given by

$$\begin{aligned} I_{fl} &= b \cdot N_i^{(L)} \cdot I_2 = b \cdot I_2 \cdot N_i^0 - a \cdot b \cdot N_i^0 \cdot I_1 I_2 \\ &= b\, N_i^0\, I_{20}(1-\cos 2\pi f_2 t) - abN_i^0 I_{10} I_{20}(1-\cos 2\pi f_1 t)(1-\cos 2\pi f_2 t) \end{aligned} \tag{2}$$

The first term represents the fluorescence induced by the probe laser in the absence of the pump laser. The second term describes the decrease in fluorescence due to the saturation of the population N_i caused by the pump laser. Evaluation of the product yields:

$$I_{f1} = b(1-aI_{20})I_{10}(1-\cos 2\, f_2 t)+abN_i^0 \cos 2\, f_1 t$$

$$- \frac{1}{2}\, abN_i^0 I_{10} I_{20} \left[\cos 2\pi(f_1+f_2)t + \cos 2\pi(f_1-f_2)t\right]$$

If the fluorescence is monitored through a lock-in amplifier, tuned to the sum frequency $(f_1 + f_2)$ only the double resonance signals are detected, while the fluorescence, induced by the pump laser or the probe laser alone can be monitored at the frequencies f_1 and f_2 respectively.

Figure 5, which shows a section of the excitation spectrum of NO_2 around $\lambda \approx 488$ nm, illustrates the complexity of the spectrum.[6] There is no regular pattern to be recognized. The OODR-method is helpful in assigning the spectrum. The lower trace of Fig. 6 reproduces a small part of the spectrum of Fig. 5. If the pump laser is stabilized on line No. 4 and the probe laser is tuned,[7] the OODR-spectrum, shown in the upper trace is obtained at the sum frequency, which proves that lines No. 1 and No. 4 share a common lower level. The separation of these two OODR-signals represents the energy separation of two upper levels m_1 and m_2, which are both optically connected with the common ground state level. Further studies showed that also the line pairs 2 and 5 and 3 and 6 were coupled by a common lower level, and that the lines 1, 2, 3 and 4, 5, 6 represent the three hyperfine structure components of two rotational transitions $(J_i'', K_i'') \rightarrow (J_m', K_m')$ with m = 1, 2.

Since the Doppler-width is reduced by a factor $\varepsilon \approx 100$, which equals the collimation ratio of the molecular beam, simultaneous excitation of several pump transitions can be eliminated. At the low pressures in the molecular beam collisions can be neglected. Therefore the combination of Doppler-free

excitation with double-resonance techniques simplifies the OODR-spectrum and makes its assignment straight forward, provided the pump transition is known.

III. Stepwise Excitation

The second OODR-scheme of Fig. 1b has proved to be very successful for the study of highly excited molecular states. The first laser populates a selected level in an excited state and the second laser induces transitions from this level into higher states. The final levels m reached by absorption of two photons, have the same parity as the initial ground state level i. This OODR excitation, which may be regarded as a resonant two photon transition, therefore gives complementary information compared with ultraviolet absorption spectroscopy where states with comparable energy but opposite parity may be reached by absorption of one ultraviolet photon.

The second transition K → m of the OODR can be monitored in different ways: when the fluorescence induced by the second laser is detected as a function of the wavelength λ_2 of the second laser, one obtains the excitation spectrum of the transitions K → m. If the states m are high lying molecular Rydberg states, they may autoionize and the number of ions detected as a function of λ_2 is a measure for the transition K → m. Another method, called "polarization labelling" is based on the orientation of the optically pumped molecules in level K. If the sample is placed between two crossed polarizers, linearly polarized light will only pass the second polarizer if its plane of polarization is being turned through the interaction with these oriented molecules (see ref. 2 on polarization spectroscopy). Only those wavelengths are therefore transmitted to the detector which coincide with transitions K → m or i → m. If the probe light is broadband radiation, generated for example by a broad-

band nitrogen laser pumped dyelaser, all transitions $k \rightarrow m$ within the bandwidth of the probe can be detected simultaneously with a photoplate or an optical multichannel analyzer (see below).

The intermediate levels K have radiative lifetimes ranging from a few ns to several μs. When pulsed lasers with pulse durations of 1 - 10 ns are used, typical for nitrogen laser pumped dyelaser, even the shorter lifetimes of some ns rise no problems. The double resonance signal S is given by

$$S = a \cdot N_i \cdot B_{iK} \cdot I_1 \cdot B_{Km} \cdot I_2 \cdot dV \qquad (4)$$

as long as saturation is avoided. Since the molecules do not travel far during the short pump pulse duration, the signal is proportional to the density N_i times the pumped volume dV.

The peak powers of pulsed dye lasers readily reach several KW and are therefore sufficiently high to saturate the transition $i \rightarrow K$. This implies that nearly 50% of the unsaturated initial population N_i can be transferred to level k. The probability P_{km} for further excitation to higher levels m by the second laser with energy density ϱ_2 at the location of the sample is

$$P_{km} = \frac{B_{km}\,\varrho_2}{B_{km}\,\varrho_2 + \Sigma\, A_{kn}} \qquad (5)$$

where B_{km} is the Einstein coefficient for absorption on the transition $k \rightarrow m$ and $\Sigma\, A_{kn}$ represents the transition probability for spontaneous decay of level k into lower levels n.

Although the transition probability for transitions $k \rightarrow m$ to higher Rydberg levels m decreases with increasing principal quantum number of these levels, pulsed lasers have sufficiently high energy densities ϱ to make $B_{km}\varrho_2 \gg \Sigma\, A_{km}$. The probability P_{km} then approaches unity. Under such favorable conditions the detection of OODR-signals imposes no serious problems.

The situation is different when cw lasers are used. Since their output powers are much smaller than the peak powers of pulsed lasers, the probability P_{km} may be much smaller than unity, which means that only a small fraction of all molecules in level k can be further excited.

The application of cw lasers to stepwise excitation of molecules faces another problem, related to the short spontaneous lifetime τ of many molecular levels k. Let the two collinear laser beams have a common diameter d. When a molecule in level i diffuses into the pump beam, it may be excited into level k at a position x. During its spontaneous lifetime τ it travels a mean distance $\bar{s} = \tau\bar{v}$, where $\bar{v}$ is the mean thermal velocity. Only that small part of the spatially distributed probe laser power between x and $x + \bar{s}$, that is "seen" by the excited molecule before it decays, is useful for further excitation $k \rightarrow m$. After the molecule has spontaneously decayed, it is lost for the pumping processes because only the small fraction $\eta = A_{ki} / \sum_n A_{kn}$ of all spontaneous decays terminates on the initial level i and can be pumped again. Most of the molecules decay into other levels n which are not optically connected with level i and could only return to it by collisional transfer.

In order to illustrate this problem, let us consider a typical example: with $\bar{v} = 500$ m/s and $\tau = 10^{-8}$ s we obtain $\bar{s} = 0.5$ μm. When the two focussed laser

beams have beam waists of w = 0.1 mm, the excited molecule travels on the average less than 0.5% of the probe beam diameter. This means that only a small fraction of the spatially distributed probe power is useful to induce the double resonance transition k → m.

For OODR-spectroscopy in molecular beams with cw lasers the geometrical arrangement of the two laser beams is of crucial importance for the optimization of the OODR-signals. The intensity of the first laser should be sufficiently high to insure that all molecules which pass through the laser beam, can be excited. On the other hand, however, it should not exceed an upper limit, to prevent that the molecules are already excited before the maximum of the Gaussian beam profile where the second laser has not sufficient power to compete with the spontaneous decay. In any case the second laser should have more power than the first and both diameters should be not much larger than the mean path $\bar{s}$. Since the molecular beam width is of the order of 1 mm, the focussing by spherical lasers would make the laser beam diameter much smaller than the molecular beam diameter and most of the molecules would pass outside the laser beam without being pumped. The most efficient geometrical arrangement for two step excitation with cw lasers in molecular beams uses a combination of spherical and cylindrical lenses [8] to focus the two collinear laser beams into a thin sheet of light with an elliptical cross section at the intersection with the molecular beam (see Fig. 7).

IV. Two Step Resonance Ionization Spectroscopy

The optimization of stepwise excitation is of particular relevance for the development of a very sensitive detection method, called two photon resonance ionization spectroscopy (see the paper by G.S. Hurst). This method is based on the OODR-scheme of Fig. 1b where the upper states m are either continuous states above the ionization limit or high lying molecular Rydbergstates which can autoionize. The molecular ions generated by the second laser on the transition k → m = k → I are used to monitor the absorption of the first laser since they are only produced from excited states k, populated by the first laser.

In this scheme the wavelength of the second laser is kept fixed and that of the first laser is tuned. Any time the first laser wavelength coincides with a transition i → k, the second laser produces ions, provided $h\nu_2 > (IP - E_k)$. The number of ions n_{ion} produced per second, is

$$n_{ion} = N_k \cdot P_{kI} = n_a \frac{P_{kI}}{P_{kI} + \sum_n A_{kn}}$$

$$= n_a \frac{B_{kI} \varrho_2}{B_{kI} \varrho_2 + \Sigma A_{kn}} \qquad (6)$$

$$= N_i \cdot \sigma_{ik} \cdot (P_1/h\nu_1) \cdot \Delta x \; \frac{B_{kI} \varrho_2}{B_{kI} \varrho_2 + A_k}$$

where n_a is the number of pump laser photons $h\nu_1$, absorbed per second at a pathlength Δx on the transition i → k at an incident power P_1, and B_{kI} is the Einstein coefficient for the transition from level k into the ionization state and $A_K = \Sigma A_{kn}$ is the total relaxation rate of level k. Equation (6) shows,

the quadrupol moment of the molecular core and its polarizability determines the actual quantum defects which depend on the electrons' angular momentum, its principal quantum number n and also slightly on the internuclear separation R [14].

The necessary condition for autoionization of a Rydberg level $E^*_n(v^*,J^*)$ into an ionic level $E^+(v^+,J^+)$ can be expressed by the energy relation

$$E^*_{vib}(v^*) + E^*_{rot} > \Delta E + E^+_{vib}(v^+) + E^+_{rot}(J^+) \qquad (8)$$

where $\Delta E = E^+(R_e) - E^*_n(R_e)$ is the energy separation of the minima of the two potential curves at the equilibrium internuclear distance R_e.

The probability for auto-ionization depends on the coupling between nuclear motions and electronic energy since part of the rotational-vibrational energy must be converted to the Rydberg electron in order to give it sufficient energy to leave the core. The auto-ionization process for Rydberg states of molecules is therefore certainly much slower than that of doubly excited atomic states. In order to estimate its efficiency one has to take into account all other possible decay channels of the excited Rydberg-state $E^*_n(v^*,J^*)$. The auto-ionization process competes with the radiative decay of the Rydberg levels and often also with possible predissociation. However, the spontaneous transition probability decreases approximately with n^{-3}. For large principal quantum numbers n, the radiative decay therefore becomes very slow and in absence of predissociation even small auto-ionization probabilities may already result in complete ionization of the Rydberg level. Since the ion can be detected with high efficiency, this makes auto-ionization by two-step excitation a very sensitive variation of resonant two photon ionization, because the transition probability for the second step $k \rightarrow n(v^*,J^*)$ is much higher than that of direct transitions $k \rightarrow I$ into the ionization continuum.

Several groups [15-18] have started experimental work on two step autoionization of diatomic molecules. Our group in Kaiserslautern [19] has chosen the Li_2-molecule because there exist very accurate calculations of ab initio potential curves [20] which can be compared with the experimental results. The experimental procedure is illustrated in Fig. 10. The Li_2 molecules are prepared in a supersonic beam which is crossed perpendicularly by two collinear laser beams from two pulsed dye lasers L1 and L2, pumped by the same nitrogen laser. The first laser L1 pumps the Li_2 molecules from a level (v''_i, J''_i) in the $X^1\Sigma^+_g$ ground state into a selected level (v'_k, J'_k) of the $B^1\Pi_u$-state. Since the molecular constants of both states are known [19a] the pump transition $(v''_i,J''_i) \rightarrow (v'_k,J'_k)$ can be assigned by observing the laser induced fluorescence. When the pump laser L1 is stabilized onto this transition, the second laser L2 is switched on and induces transitions from the intermediate level (v'_k,J'_k) into higher Rydberg levels (v^*,J^*), which can auto-ionize. The number of ions is monitored as a function of the wavelength λ_2 of L2, at first with L1 off and then with L1 on. The difference between the two readings gives those ions which are produced by L2 on a transition $(v'_k, J'_k) \rightarrow (v^*,J^*)$ or by direct photoionization

$$Li_2(v'_k, J'_k) + h\nu_2 \rightarrow Li_2^+ + e^- \qquad (9)$$

In our experiment $2h\nu_2$ was larger than the ionization limit of $Li_2(X^1\Sigma_g)$. The second laser alone can therefore also produce ions by two photon ionization.

The probability for this process is, however, sufficiently large only for resonant two photon ionization when the photon energy $h\nu_2$ fits to a molecular transition

$$Li_2(X^1\Sigma_g(v'',J'')) + h\nu_2 \rightarrow Li_2\ B^1\Pi_u(v_2',J_2') \qquad (10)$$

The middle trace (a) in Fig. 11 shows the number of ions $N_{ion}(2\nu_2)$ produced with L1 off. The peaks correspond to resonant transitions(10), as could be proved by observation of the corresponding fluorescence (lowest trace in Fig. 11B).When the pump laser L1 is switched on, the upper trace (b) in Fig. 11 is recorded. The difference between the two curves (note that the upper curve is vertically shifted by an amount indicated by the arrow in order to separate the two recordings) gives the number of ions produced by one photon $h\nu_2$ on a transition from a labelled level (v_k',J_k') in the intermediate state. The auto-ionization lines can be seen superimposed on a continuum which increases with decreasing wavelength λ_2. The continuum is attributed to the direct photoionization process (8) and from its onset at λ_2 = 474.9 nm, measured at different electric field strengths, the adiabatic ionization potential

$$IP = E(X^2\Sigma_g^+,\ v^+ = 0,\ J^+ = 0) - E(X^1\Sigma_g^+,\ v'' = 0,\ J'' = 0) \qquad (11)$$

is determined to be $IP(Li_2) = 41475 \pm 8\ cm^{-1}$. A comparison between Figs. 11A and 11B shows that with increased strength of the electric field used to extract the ions, some new auto-ionization lines appear close above the ionization threshold. They can be attributed to very high Rydberg levels with $n \cong 50$ and $v^* = 0$ which auto-ionize by rotational coupling into $v^+ = 0$. The molecules in these levels have a large polarizability and the induced dipole

moment may enhance the coupling efficiency.

The linewidth of the auto-ionization lines is very narrow and mainly determined by the laser bandwidth of about 3 GHz. In order to investigate the linewidth in more detail, the bandwidth of L2 was reduced to 1.5 GHz by inserting an extra etalon into the laser cavity. The laser linewidth could be determined from the width of the lines $I_{FI}(\lambda_2)$ induced by L2. Figure 12, which shows two auto-ionization lines excited at two different field strengths, illustrates that the linewidth increases with increasing electric field. The steps in the line profiles are due to the stepwise scanning of the laser wavelength. From a comparison of these line profiles with the fluorescence line profiles excited by the same laser, an upper limit $\Delta\nu \leq 300$ MHz for the auto-ionization linewidth at low fields can be obtained. This implies that the lifetime of the auto-ionizing state is at least 0.5 ns, probably longer [20].

Compared to atomic auto-ionizing states, where lifetimes below 10^{-12} s are common, the molecular levels exhibit a much weaker coupling to the ionization continuum. The reason is that the molecular ionization process takes place through a coupling between nuclear motion and electronic configurations, whereas in atoms a direct electronic coupling of the excited electron to the continuum makes the auto-ionization probability by far larger.

Similar experiments on auto-ionization of molecular Rydberg levels have been performed on Na_2 and K_2 by Martin et al. [17] and by Leutwyler et al. [18,21]. A complete analysis of the auto-ionization spectra of all these alkali molecules is, however, still pending since a full understanding of all perturbations requires very detailed studies of the many molecular states closely

below the ionization limit. These may be not only Rydberg states but also doubly excited states which dissociate into A* + B*. These states can perturb the Rydberg states and congest the spectra.

Several groups have attacked these problems. Bernheim et al. [21] have performed OODR spectroscopy of Rydberg states of Li_2 below the ionization limit. The probe transitions were monitored through the fluorescence excited by the probe laser. For a given intermediate level (v', J') of a Σ-state, there are not only P- and R-lines with $\Delta J = \pm 1$ possible for transitions to Σ - Rydberg states but also simultaneously P, R and Q-lines to π Rydberg states. Because of perturbations, including l-uncoupling phenomena [22] the assignments of the different lines is not obvious. The authors succeeded, however, to assign several Rydberg series [23].

Here double-resonance polarization spectroscopy is very helpful because it allows one to distinguish between P, Q or R-transitions[2]. Schawlow et al. [24,25] have investigated many Rydberg states of Na_2 by this technique. They used a narrow band pulsed pump laser to label selected intermediate levels (v',J'), and recorded with a broadband probe laser many OODR transitions simultaneously on a photographic plate (polarization labelling technique [26]). The technique is also applicable with cw lasers and photoelectric recording with the advantages of sub-Doppler resolution and higher accuracy of wavelength measurements.

Detailed sub-Doppler OODR spectroscopy of BaO has been performed by W. Field and coworkers [27], who used the stepwise excitation scheme of Fig. 1b. The resonance transitions k → m of the probe laser were monitored by the decrease

of the fluorescence intensity, emitted from level k, as well as by the appearance of a new, ultraviolet fluorescence, emitted from the level m into the electronic groundstate. This method not only allowed a precise characterization of excited electronic states of BaO in the 4 eV region, but also of low lying metastable states.

VII. OODR-Spectroscopy of Dissociating States

Most spectroscopic efforts are directed towards bound states since they give rise to line spectra which allow one to determine molecular constants and potential curves. Much less is known about repulsive states, which are responsible for continuous spectra. They sometimes make themselves conspicuous in discrete spectra by predissociation of bound states which results in broadening of spectral lines. If sufficient predissociating levels can be found, the potential curve of the repulsive states can be sometimes deduced, at least for a certain range of internuclear distances R. However, in many cases it is not clear into which atomic state the repulsive potential curves dissociate.

Collins et al. [28] used a very elegant variation of OODR-spectroscopy to scan repulsive potential curves of excited states (AB)* and detect the excited atomic states A* into which they dissociate. The method is illustrated in Fig. 13. A pulsed tunable dye laser is scanned through the molecular spectrum of interest. The pulse from the second dye laser is sent through the sample cell with a short delay. Its wavelength is tuned to the atomic transition between the excited state A* and a higher atomic Rydberg state A**. When the first laser excites a repulsive molecular state (AB)* that dissociates into A* + B, the second laser can further excite the atoms A* produced by photodissociation

into the state A** closely below the ionization limit. The sample cell is built as thermonic detector where the excited atoms A** are ionized by collisions with electrons and are detected with the space charge amplification technique (see chapter V).

The signal, measured at a selected atomic transition (λ_2 = const) as a function of λ_1 yields the probability for transitions from the molecular groundstate to the repulsive state. This allows one to determine the wave function of the repulsive state and its potential curve.

The power of this "photolytic spectroscopy" was demonstrated by applying it to the spectroscopy of repulsive states of Cs_2 [29]. Fig. 13 shows the corresponding potential diagram. The authors found different repulsive states which dissociate into the atomic Cs states $6P_{1/2}$, $6P_{3/2}$, $5D_{3/2}$ and $5D_{5/2}$ and which overlap in their spectral excitation ranges.

VIII. Accurate Determination of Dissociation Energies by OODR

In the A-type OODR scheme of Fig. 1c pump and probe transitions share a common upper level. Of particular interest are those probe transitions k → m that terminate on high vibrational levels m = (v", J") of a lower electronic state or on the continuum above the dissociation limit. Since levels with sufficient energy above the lowest level v" = 0 have negligible populations at thermal equilibrium, the probe wave may even experience gain rather than absorption, provided the upper level k is appreciably populated by the pump transitions. In a proper resonator configuration even laser oscillation can be achieved on these transitions if the total gain overcomes the losses [30]. In this section

we briefly discuss applications of the A-type OODR scheme to the accurate determination of dissociation energies.

Assume the pump laser excites a high vibrational level v' in an upper electronic state k, less tightly bound than the groundstate. The potential minimum of this state will then be found at a larger internuclear separation R_e than that of the groundstate. When the pump transition starts from a low, thermally populated vibrational level in the groundstate i, the maximum Franck-Condon factors occur for those vertical transitions which reach the upper state at the inner limb of the potential curve (see Fig. 14). The excited molecule undergoes many vibrations during its spontaneous lifetime and the fluorescence can be in principle emitted at any value of R within the inner and outer turning points R_i and R_o. However, if vertial transitions from the outer turning point can reach the outer part of the groundstate potential, these transitions will have the largest Franck-Condon factors because the vibrating molecule spends a longer time near the outer turning points.

Under such conditions where the upper potential curve is shifted against the lower towards larger internuclear separations, the fluorescence spectrum shows, besides intense transitions between the inner repulsive parts of the potentials around the excitation wavelength, even stronger transitions terminating on very high vibrational levels of the lower state i. Also bound-free continuous fluorescence spectra are found which represent transitions from the upper level (v',J') in state k into continuous states above the dissociation limit [31].

The long wavelength section of such a fluorescence spectrum of Cs_2, as excited

by a single mode dye laser on the transition $X^1\Sigma_g^+(v''=0, J''=49) \rightarrow D^1\Pi_u^+(v'=50, J'=48)$ is shown [32] in Fig. 15. From the rotational spacings $\nu(v'',J''=J'-1) - \nu(v'',J''=J'+1)$ of P and R lines, and from the vibrational spacings $\nu(v''+1,J'') - \nu(v'',J'')$ of lines, terminating on high vibrational levels v" closely below the dissociation limit, the accurate determination of the dissociation energy D_e is possible [33]. For the Cs_2 molecule we obtained from the fluorescence spectrum a value $D_e(^1\Sigma_g^+) = 3648 \pm 8\ cm^{-1}$. From the structure of the continuous fluorescence spectrum the difference potential $V_k(R) - V_i(R)$ can be deduced [31].

The spectral resolution of the fluorescence lines which is determined by the monochromator, used to disperse the spectrum, is not high enough to separate the rotational lines for high values of v" since their spacings $4B_{v''}(J'+1/2)$ decrease rapidly with increasing v". Here the OODR spectroscopy offers much higher resolution and allows one to resolve rotational spacings very close to the dissociation limit, even when they become narrower than the Doppler-width.

Figure 16 demonstrates the signal to noise ratio of OODR signals obtained with polarization spectroscopy of the Cs_2 molecule. The signal P(72) represents an OODR transition according to the V-scheme of Fig. 1a, where pump and probe transitions share a common lower level. The line P(74) represents a A-type OODR signal according to Fig. 1c where the upper level J' = 73 is shared and the probe transition is due to stimulated emission rather than absorption. Pump- and probe-waves were travelling antiparallel through the sample.

The small signals P(70) and P(76) in Fig. 16 are secondary OODR signals, caused by collisional population transfer within the lower state from levels J"=70 and 76 to the depleted level J"=72. Note, that in homonuclear diatomic molecules collisions can only induce rotational transitions with even ΔJ values because of symmetry selection rules.

High vibrational levels in excited electronic states can be probed by triple resonance spectroscopy first applied to the Na_2 molecule by R. Field and his coworkers [34]. The technique which is also called "modulated gain spectroscopy" is illustrated by Fig. 17. A single mode dye laser excites the molecules into higher vibrational levels v' in the A- or B-state. With sufficient pump power, inversion can be reached between v' and high lying levels v" of the ground state. The resulting optically pumped "dimer-laser" populates these levels by stimulated emission. A second dye laser is now tuned to a transition between these high v"-levels and very high v' levels in the A- or B-state. When the first dye laser is chopped, so will be the dimer laser intensity and with it the population $N(v''_m)$ of the terminating level, commom to dimer laser and second dye laser.

These experiments can give information on the exact form of the potentials V(R) in a range of internuclear distances R where the pure van der Waals potential $V(R) = C\ R^{-6}$ already fails but quantum-mechanical calculations, which give optimum results around the potential minimum, are not sufficiently accurate. In particular they can investigate the influence of spin-orbit coupling in the intermediate range between Hunds coupling cases (a) and (c) by accurately measuring for example the potential curves of molecular singulet and triplet states dissociating into the same atomic doublet states.

IX. OODR Spectroscopy Below the Natural Linewidth

When the two beams of pump laser and probe laser in the OODR scheme of Fig. 1c travel collinearly instead of antiparallel, a particular situation arises. The molecule interacts simultaneously with two copropagating waves which are both in resonance with two coupled molecular transitions. This may be regarded as a resonant stimulated Raman scattering process, where the characteristic features of the intermediate level k, such as its lifetime and levelwidth, do not enter into the linewidth of the Raman signal. It can be shown [35] that for this case the linewidth γ_{DR} of the double resonance signal is given by

$$\gamma_{DR} = \gamma_i + \gamma_m + \left(1 - \frac{k_{probe}}{k_{pump}}\right) \gamma_k \qquad (12)$$

where k denotes the wavevector of the probe wave and pump wave. If both waves travel collinearly, $k_{pump} \parallel k_{probe}$ and the last term in (12) becomes very small. For $\lambda_{pump} = \lambda_{probe}$ it becomes zero.

When the levels i and m are rotational-vibrational levels of the electronic groundstate, they have long radiative lifetimes τ (for homonuclear molecules τ even becomes infinite). The level widths γ_i and γ_m are therefore small compared to γ_k. For homonuclear molecules the width γ_{DR} of the double resonance signal becomes a small fraction of the width γ_k of the upper level

$$\gamma_{DR} = (1 - \lambda_{pump}/\lambda_{probe})\, \gamma_k$$

The Λ-type OODR spectroscopy with copropagating beams therefore allows a spectral resolution which goes beyond the natural linewidth γ_k of the optical transitions $i \rightarrow k$ or $k \rightarrow m$.

The technique has been applied by Ezekiel et al. [36] to the I_2 molecule. The optical transitions, choosed in this case, have , however, a very small natural linewidth of approximately 100 KHz. Because of laser frequency jitter, time of flight broadening and other broadening effects, it is therefore very hard to obtain linewidths below 100 KHz. The authors could, however, show that the width γ_{DR} of the double resonance signal was much smaller for copropagating pump- and probe waves than for counter propagating waves.

M. Raab [37] has performed OODR-polarization spectroscopy of the Cs_2 molecule. Here the spontaneous lifetimes are a few ns and the natural linewidth is about 20 MHz, which makes it easier to observe subnatural linewidths. Figure 18 shows two double resonance signals in the polarization spectrum of Cs_2, which are generated with a fixed pump laser, stabilized on a transition $X^1\Sigma_g^+(v''=4, J''=104) \rightarrow C^1\Pi_u(v'=5, J'=105)$, and a tunable probe laser. Both laser beams propagate nearly collinearly. The left OODR signal corresponds to the V-type scheme of Fig. 1a, the right signal to the Λ-type scheme of Fig. 1c. Both signals have residual Doppler-widths of about 6 MHz due to the finite crossing angle of 0.01 rad between the two beams. Together with the natural linewidths of 20 MHz which is slightly power broadened to about 25 MHz, this results in a total linewidth of 28 MHz for the OODR signal of the V-type . The Λ-type signal, however, is only 18 MHz.

This subnatural OODR spectroscopy may be useful to resolve narrow level spacings of rotational levels of loosely bound molecules close to the dissociation

limit. There are predictions [38] that such molecules have potential minima at very large internuclear distances. The spacings of rotational levels will then be exceedingly narrow. The problem of rotational predissociation or the occurence of double minima potentials in diatomic molecules can be attacked with this technique.

This lecture intends to give a survey about the basic principles, experimental problems and some applications of OODR spectroscopy. Most of the examples, used to illustrate the techniques, have been taken from the work of the graduate students in my group, in particular D. Eisel, H.J. Foth, M. Raab, H.J. Vedder and H. Weickenmeier. There has been much more work performed, of course, in many other laboratories. Only a small selection of many papers has been mentioned here.

References

1) J.L. Hall: "Saturated Absorption Spectroscopy", in: Atomic Physics Vol. 3, ed. by St. Smith, G.K. Walters (Plenum Press, New York 1973), p. 615 ff.

2) M. Raab, G. Höning, W. Demtröder, and C.R. Vidal: High resolution laser spectroscopy of Cs_2: II. Doppler-free polarization spectroscopy of the $C^1\Pi_u \leftarrow X^1\Sigma_g^+$ system, J. Chem. Phys. 76, 4370 (1982)

3) H.J. Foth, H.J. Vedder and W. Demtröder: "Sub-Doppler Laser Spectroscopy of NO_2 in the λ = 592.5 nm Region", J. Mol. Spectrosc. 88, 109 (1981)

4) D.H. Levy, L Wharton and R.E. Smalley: "Laser Spectroscopy in Supersonic Jets", in: Chemical and Biochemical Applications of Lasers, Vol. II: ed. by C.B. Moore (Academic Press, New York 1977)

5) G. Herzberg: Molecular Spectra and Molecular Structure, Vol. I, p. 168 ff (Van Nostrand Reinhold Comp., New York 1950)

6) R. Schmiedl, I.R. Bonilla, F. Paech, W. Demtröder: "Laser Spectroscopy of NO_2 under very high resolution", J. Mol. Spectrosc. 68, 236 (1977)

7) W. Demtröder, D. Eisel, H.J. Foth, G. Höning, M. Raab, H.J. Vedder, and D. Zevgolis: "Sub-Doppler Laser Spectroscopy of Small Molecules" J. Mol. Structure 59, 291 (1980)

8) E. Gottwald: Diplomthesis, Fachbereich Physik, Univ. Kaiserslautern 1980
K. Bergmann and E. Gottwald: "Effect of Optical Pumping in Two-Step Photoionization of Na_2", Chem. Phys. Lett. 78, 515 (1981)

9) M. Becker: Diplomthesis, Fachbereich Physik, Univ. Kaiserslautern 1982

10) G.V. Marr and S.R. Wherrett:"The Ionization of Caesium Vapor by the Method of Space Charge Amplification", J. Phys. D, At. Mol. Phys. 5, 1735 (1972)
M.E. Koch and C.B. Collins: "Space Charge Ion-Detection of Multiphoton Absorption Phenomena in Lithium Vapor", Phys. Rev. A19, 1098 (1979)

11) K.C. Harvey and B.P. Stoicheff:"Fine Structure of the n^2D Series in Rubidium near the Ionization Limit", Phys. Rev. Lett. 38, 537 (1977)

12) W. Theiß, Diplomthesis, Fachbereich Physik, Univ. Kaiserslautern, 1982

13) A.R.W. McKellar, T. Oka, B.P. Stoicheff: "Laser Spectroscopy V, part VI" Panel Discussion on Rydberg States (Springer Series in Opt. Sciences Vol. 30, Berlin, Heidelberg, New York 1981)

14) M.J. Seaton: "Quantum Defect Theory" Proc. Phys. Soc. 88, 801 (1966) M. Raoult and Ch. Jungen: "Calculation of Vibrational Preionization by Multichannel Quantum Defect Theory", J. Chem. Phys. 74, 3383 (1981)

15) S. Leutwyler, A. Hermann, L. Wöste, E. Schuhmacher: "Isotope Selective Two-Step Photoionization Studies of K_2 in a Supersonic Molecular Beam" Chem. Phys. 48, 253 (1980)

16) S. Leutwyler, M. Hofmann, H.P. Härri, E. Schuhmacher: "The Adiabatic Ionization Potentials of the Alkali Dimers Na_2, NaK and K_2" Chem. Phys. Lett. 77, 257 (1981)

17) S. Martin, J. Chevaleyre, S. Valignant, J.P. Perrot, M. Broyer, Chabaud, A. Hoareau: " Autoionizing Rydberg States of the Na_2 Molecule" Chem. Phys. Lett. 87, 235 (1982)

18) D. Eisel, W. Demtröder: "Accurate Ionization Potential of Li_2 from Resonant Two-Photon Ionization", Chem. Phys. Lett. 88, 481 (1982)

19) D. Eisel, PhD-Thesis, Universität Kaiserslautern, 1982

19a) M.M. Hessel, C.R. Vidal: "The $B^1\Pi_u \leftarrow X^1\Sigma_g^+$ bandsystem of the $^7Li_2$ molecule", J. Chem. Phys. 70, 4439 (1979)

20) P. Botschwina, D. Eisel, W. Müller and W. Demtröder, to be published in Chem. Phys. 1983

21) R.A. Bernheim, L.P. Gold, P.B. Kelley, C. Tomczyk: "A Spectroscopic Study of the $E^1\Sigma_g^+$ and $F^1\Sigma_g^+$ States of Li_2 by Pulsed Optical-Optical Double Resonance", J. Chem. Phys. 74, 3249 (1981)

22) U. Fano: "Quantum Defect Theory of l-uncoupling in H_2 as an Example of Channel Interaction Treatment", Phys. Rev. A2, 353 (1970)

23) R.A. Bernheim, L.P. Gold and T. Tipton; J. Chem. Phys. in press (1982)

24) N.W. Carlson, A.J. Taylor and A.L. Schawlow: "Identification of Rydberg States in Na_2 by Two-Step-Polarization Labelling", Phys. Rev. Lett. 45, 18 (1980)

25) N.W. Carlson, A.J. Taylor, K.M. Jones and A.L. Schawlow: "Two-Step Polarization Labelling Spectroscopy of Excited States of Na_2", Phys. Rev. A24, 822 (1981)

26) R. Teets, R. Feinberg, T.W. Hänsch and A.L. Schawlow: "Simplification of Spectra by Polarization Labelling", Phys. Rev. Lett. 37, 683 (1976)

27) R.A. Gottscho, P.S. Weiss, R.W. Field: "Sub-Doppler Optical-Optical Double Resonance Spectroscopy of BaO", J. Mol. Spectrosc. 82, 283 (1980)

28) C.B. Collins, J.A. Anderson, F.W. Lee and P.A. Vicharelli, D. Popescu and I. Popescu: "Two-Photon Technique for the Dissociative Spectroscopy of Single Molecules", Phys. Rev. Lett. 44, 139 (1980) .

29) C.B. Collins, F.W. Lee, J.A. Anderson, P.A. Vicharelli, D. Popescu and I. Popescu: "Photolytic Spectroscopy of Simple Molecules I + II" J. Chem. Phys. 74, 1053 (1981) and 74, 1067 (1981)

30) B. Wellegehausen: Optically Pumped cw Dimer Lasers, IEEE J. Quant. Electr. QE-15, 1108 (1979)

31) J. Tellinghusen and M.B. Moeller, Chem. Phys. 50, 301 (1980)

32) M. Raab, H. Weickenmeier, W. Demtröder: The Dissociation Energy of the Cesium Dimer, Chem. Phys. Lett. 88, 377 (1982)

33) R.J. LeRoy: Energy Levels of a Diatomic near Dissociation, Molecular Spectroscopy Vol. I, Chem. Soc. Specialist Periodical Report (Chem. Soc. London 1973) pp. 113-176

34) H.S. Schweda, G.K. Chawla and R.W. Field: Highly Excited, Normally Inaccessible Vibrational Levels by Sub-Doppler Modulated Gain Spectroscopy: The Na_2 $A^1\Sigma_u^+$ State, Opt. Comm. 42, 165 (1982)

35) V.P. Chebotayev, in: V.S. Lethokov, V.P. Chebotayev, Non Linear Laser Spectroscopy (Springer Series in Opt. Sciences, Vol. 4, Springer Berlin (1979))

36) R.P. Hackel, S. Ezekiel: "Observation of Subnatural Linwidths by Two-Step Resonant Scattering in I_2-vapor", Phys. Rev. Lett. 42, 1736 (1979)

37) M. Raab, PhD-Thesis, University of Kaiserslautern 1981

38) W.C. Stwalley, Y.H. Wang, G. Pichler; Phys. Rev. Lett. 41, 1164 (1978)

Figure Captions

Fig. 1: Three possible OODR-schemes.

Fig. 2: Comparison of OODR-spectroscopy (left) with laser induced fluorescence (LIF)-spectroscopy (right).

Fig. 3: Generation of "secondary" double resonance signals by pump-laser induced fluorescence and by collisional population transfer.

Fig. 4: Experimental arrangement for sub-Doppler OODR-spectroscopy in a molecular beam under collision-free conditions. The two lasers are chopped at different frequencies f_1 and f_2 and the OODR-signals are monitored through a lock-in amplifier, tuned to the sum frequency.

Fig. 5: Sub-Doppler excitation spectrum of NO_2 around λ = 488 nm.

Fig. 6: OODR spectroscopy of NO_2. Lower spectrum: section of the sub-Doppler spectrum of Fig. 5, obtained when laser L1 is tuned. Upper spectrum: OODR-signals obtained with the pump laser L1 stabilized on line No. 4, and L2 being tuned.

Fig. 7: Optimum focussing of laser beams for stepwise excitation with cw lasers in molecular beams.

Fig. 8: OODR-signals in a Na_2 heatpipe, monitored with the space charge amplification technique. The left signal is obtained with 50 mW from a single mode Ar-laser, tunable around λ = 488 nm, and represents a resonant two-photon excitation with the Lamb-dip.

The right signal is obtained with the argon laser stabilized on the Lamb-dip and a single mode dye laser (a few mW) is scanned over a transition from the pumped level (v' = 6, J' = 46) in the B-state to a level (v*, J*) in a higher Rydberg-state.

Fig. 9: Potential curves of molecular Rydberg-states. Rotational-vibrational levels (v*, J*) of Rydberg states may autoionize if they are above levels (v^+, J^+) of the ionic ground state.

Fig. 10: Experimental arrangement for resonant two-photon ionization in a molecular beam. The fluorescence is monitored with a photomultiplier, the ions are collected by a small electric field and focussed on an open multiplier.

Fig. 11: Section of the two-step photoionization spectrum of Li_2 around the ionization threshold. Superimposed on a continuous background due to direct photoionization from the intermediate level $B^1\Pi_u$ (v' = 0, J = 6) the autoionization lines can be seen.
A: E = 50 V/cm, B: E = 20 V/cm.

Fig. 12: Linewidth of autoionizing lines at different electric fields used to extract the ions.
a) E = 20 V/cm, b) E = 100 V/cm. The lower curves in a) and b) are recorded with the pump laser off.

Fig. 13: Potential diagram of Cs_2 for illustration of photolytic double resonance spectroscopy.

Fig. 14: Schematic potential diagram for the excitation of high vibrational levels with subsequent fluorescence to levels close to the

dissociation limit. The dashed curve represents the difference potential.

Fig. 15: Laser induced fluorescence spectrum of Cs_2, excited on a transition $X^1\Sigma_g^+(v'' = 0, J'' = 49) \rightarrow D^1\Sigma_u(v' = 50, J' = 48)$ and terminating on high vibrational levels of the X ground state. The modulated continuum is due to fluorescence terminating in the continuum above the dissociation limit.

Fig. 16: OODR signals obtained with double resonance polarization spectroscopy of Cs_2. The level scheme illustrates the two signals P(72) (scheme of Fig. 1a) and P(74) (scheme of Fig. 1c). Pump and probe beams are antiparallel. The small signals P(70) and P(76) are collision induced "secondary" double resonance signals.

Fig. 17: Excitation schemes for the investigation of high vibrational levels in excited states of Na_2 by modulated gain spectroscopy.

Fig. 18: Two OODR signals with collinear pump and probe beam. Left signal: scheme of Fig. 1a, right signal: scheme of Fig. 1c. Note the smaller linewidth of the left signal which is below the natural linewidth of the optical transition.

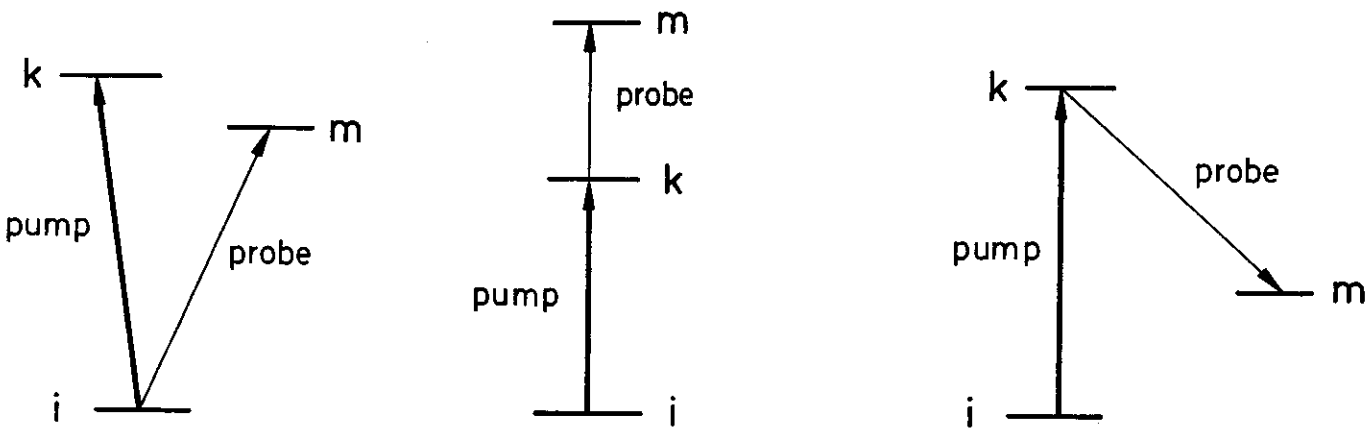
k
m
pump
probe
i
a
m
probe
k
pump
i
b
k
probe
pump
m
i
c

FIG.1

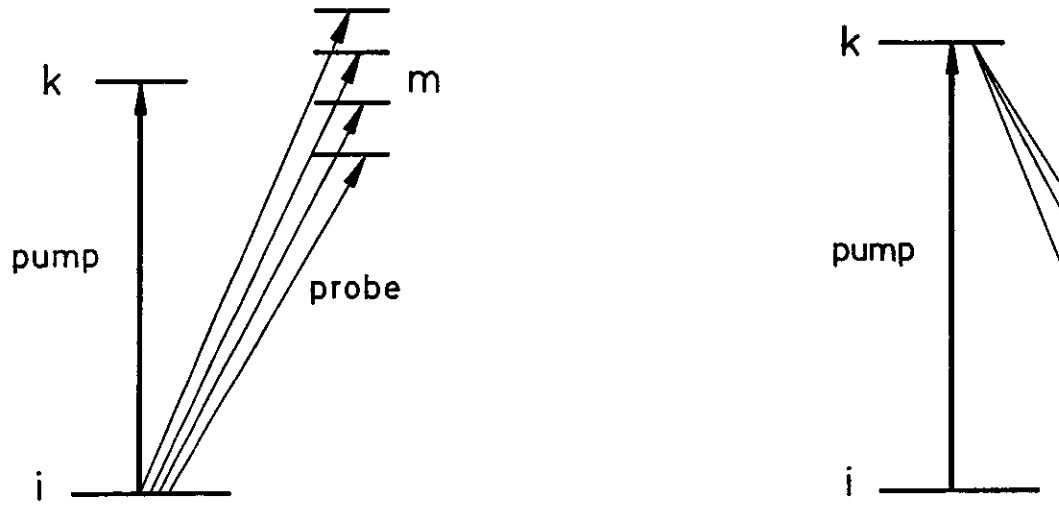
k
m
pump
probe
i
OODR
k
fluorescence
pump
m
i
LIF

FIG.2

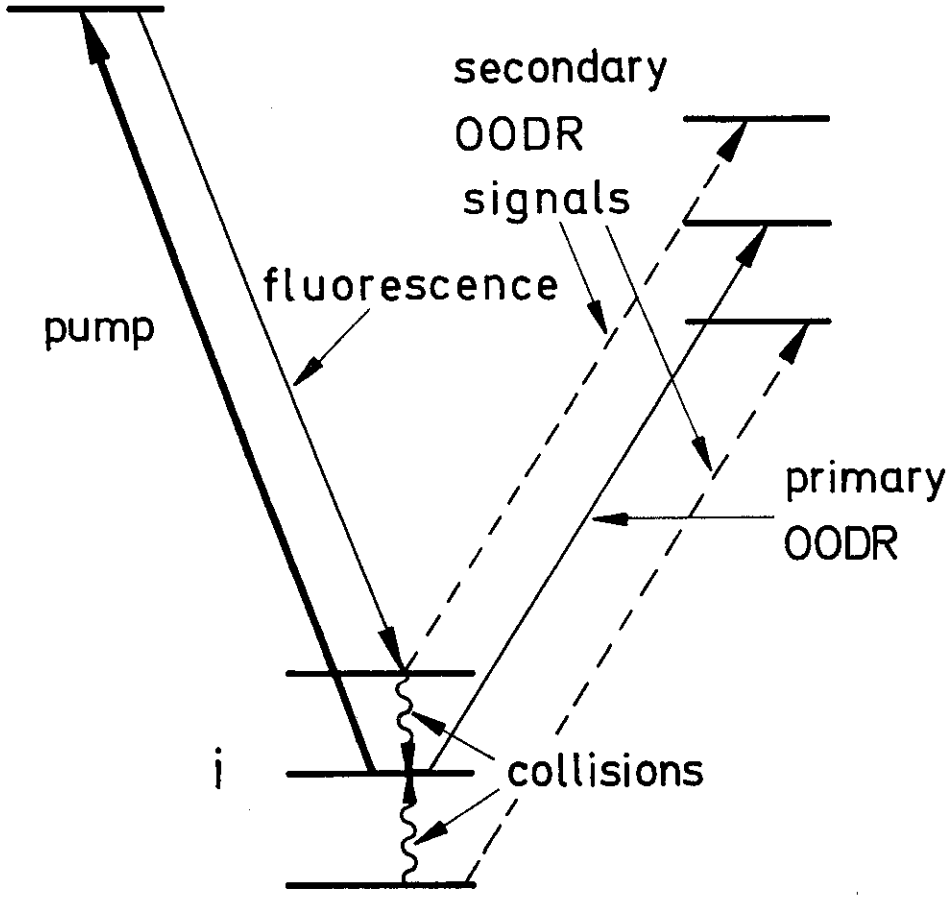

FIG. 3

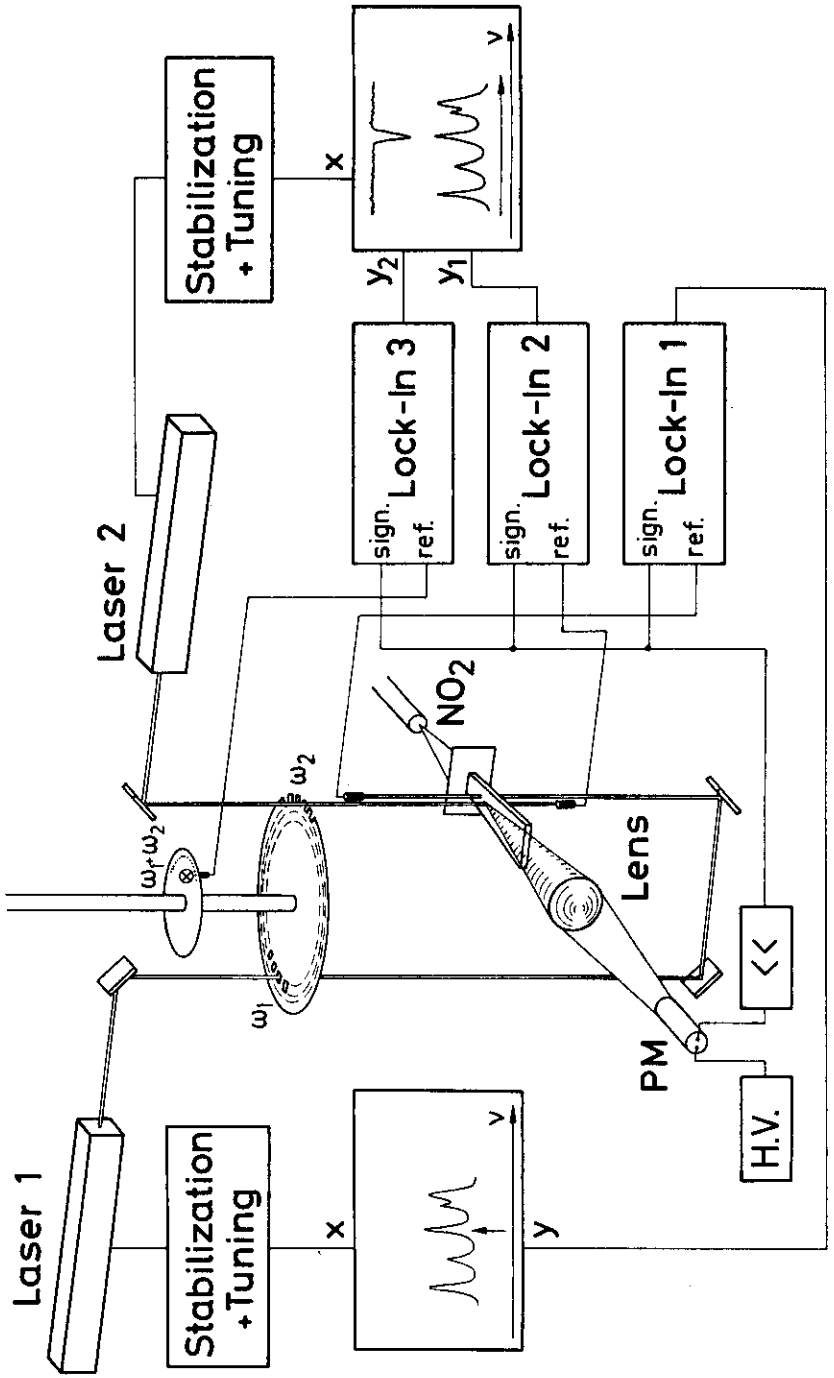

FIG. 4

Fig.3

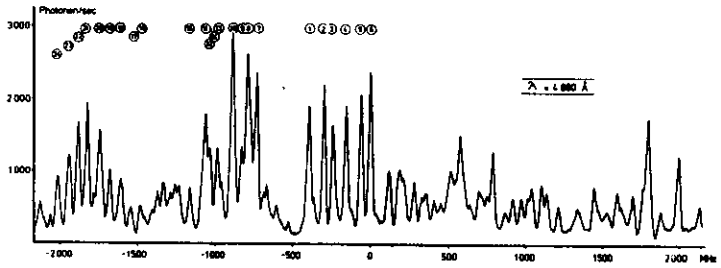
Photonen/sec
3000
2000
1000
-2000
-1500
-1000
-500
0
500
1000
1500
2000 MHz

Fig. 5

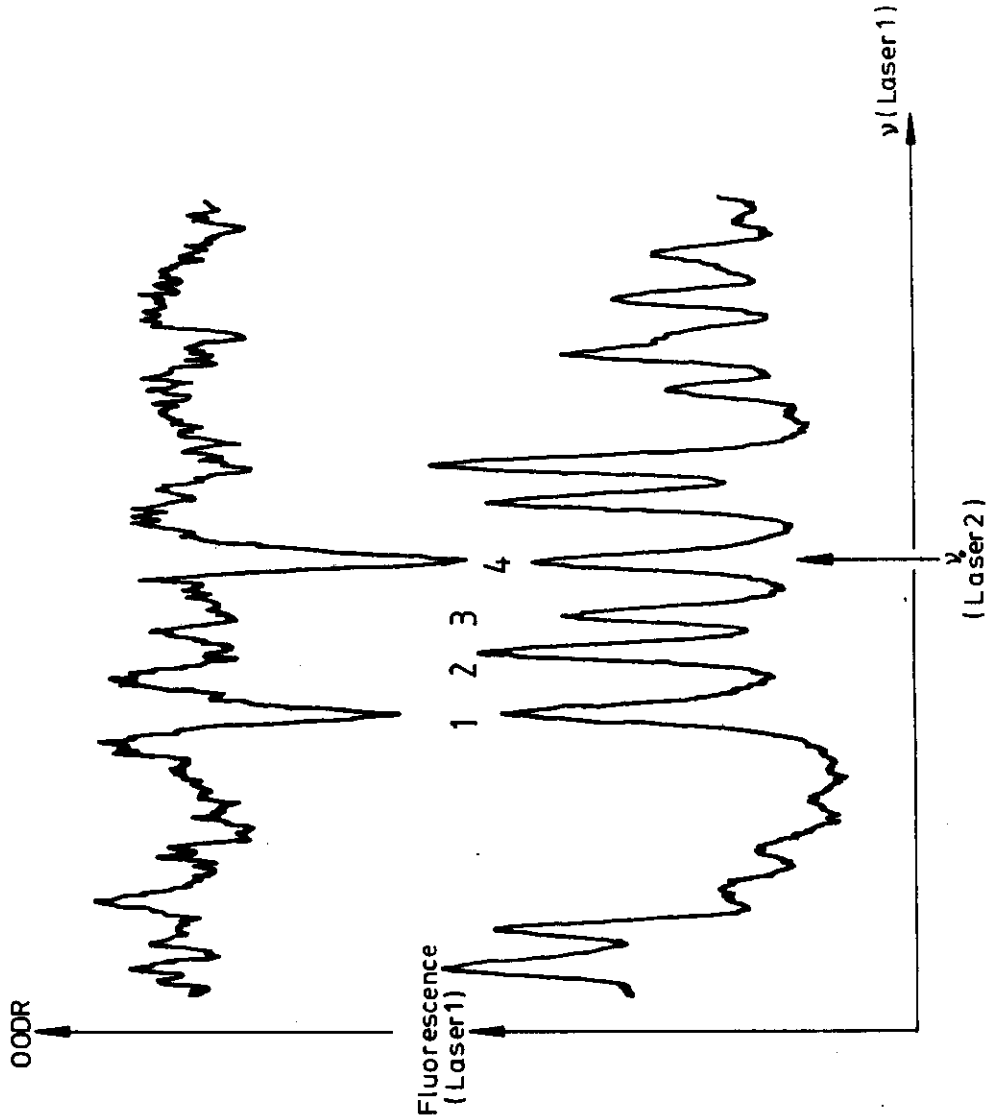
ν (Laser 1)
ν (Laser 2)
1
2
3
4
ODDR
Fluorescence (Laser 1)

Fig. 6

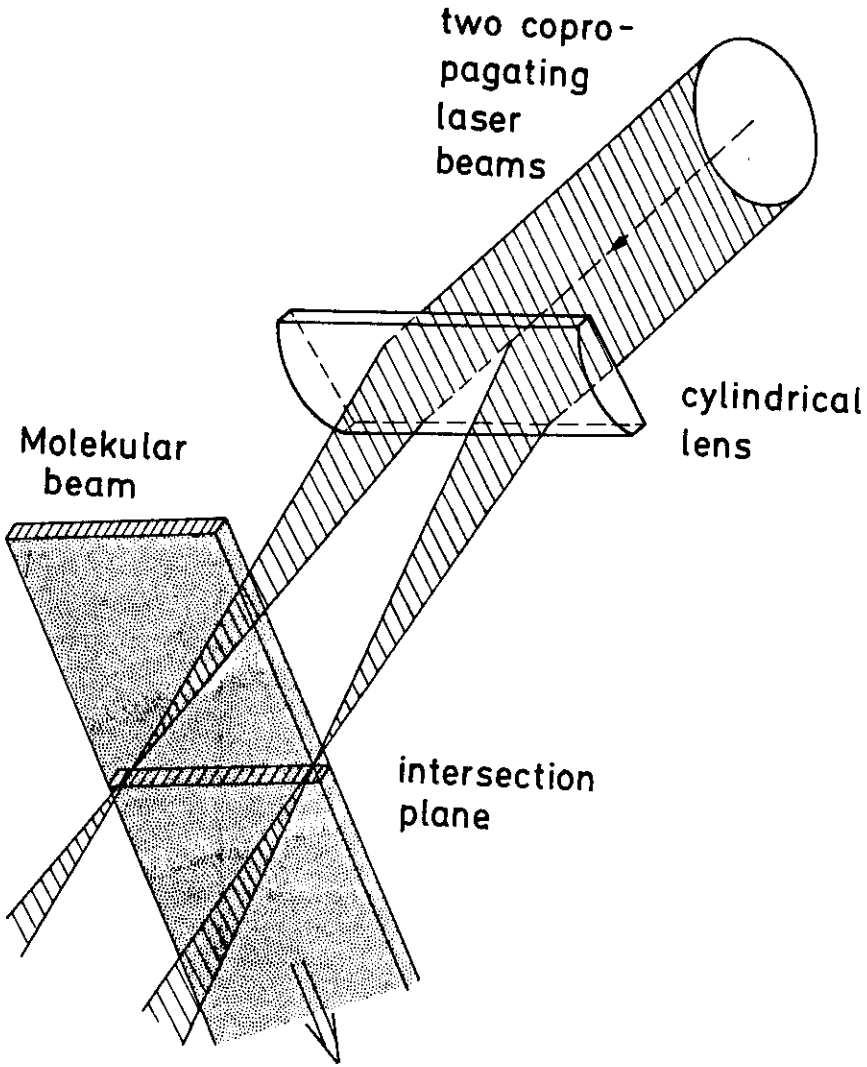
two copro-
pagating
laser
beams
cylindrical
lens
Molekular
beam
intersection
plane

Fig. 7

Fig. 8

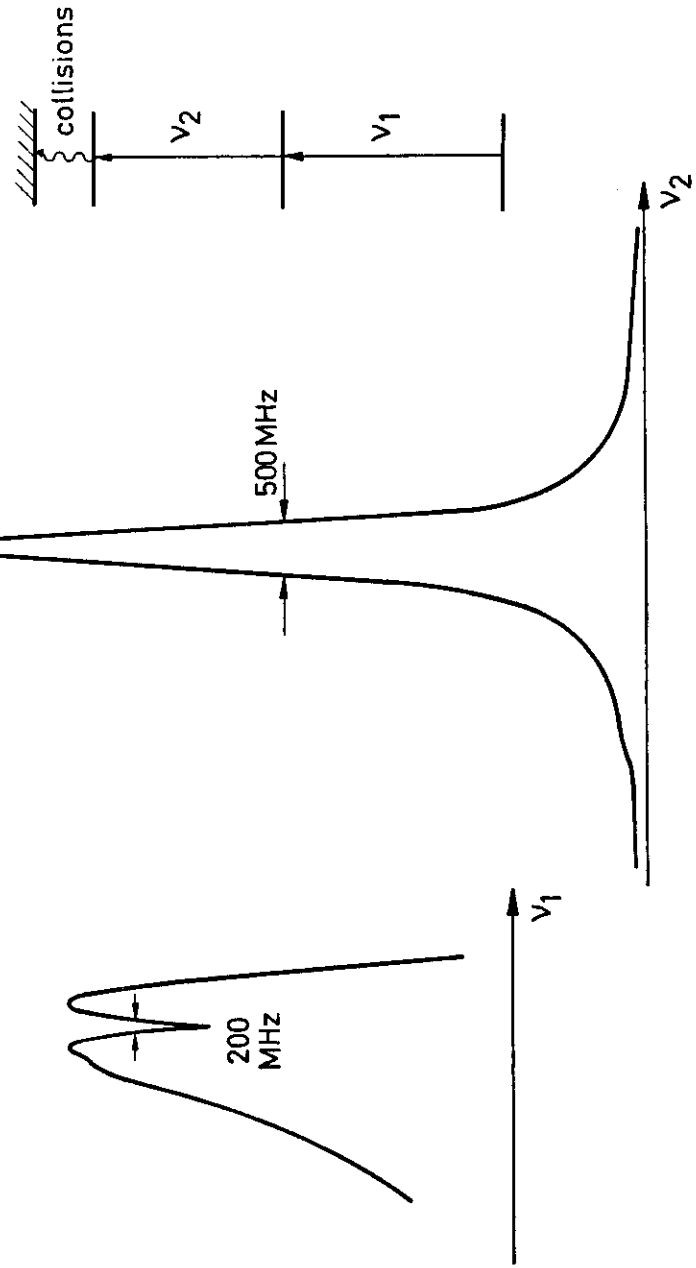
collisions
ν_2
ν_1
ν_2
500 MHz
ν_1
200
MHz

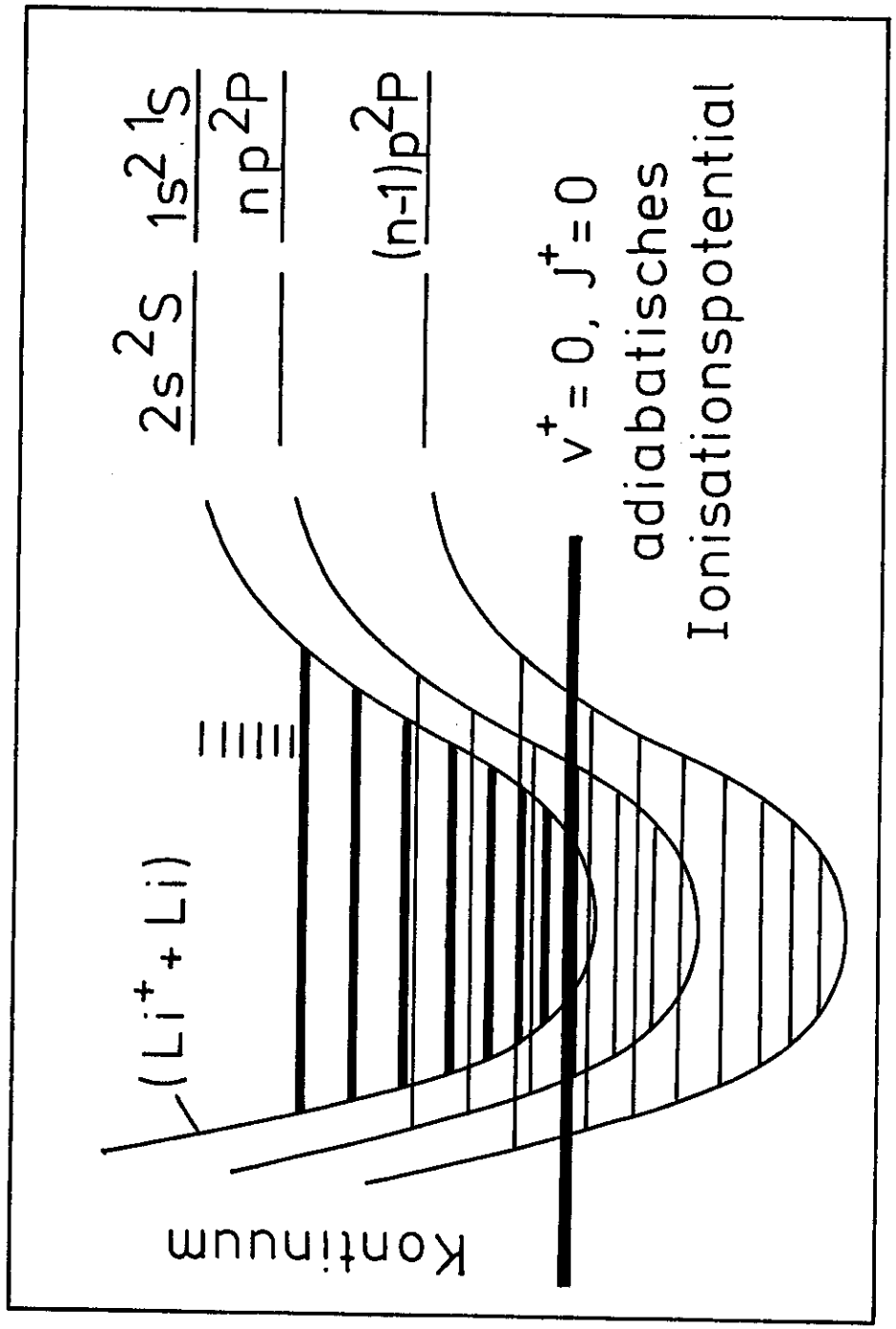
2s 2S
1s2 1S
np 2P
(n-1)p 2P
v+ = 0, J+ = 0
adiabatisches Ionisationspotential
(Li+ + Li)
Kontinuum

Fig. 9

Fig. 10

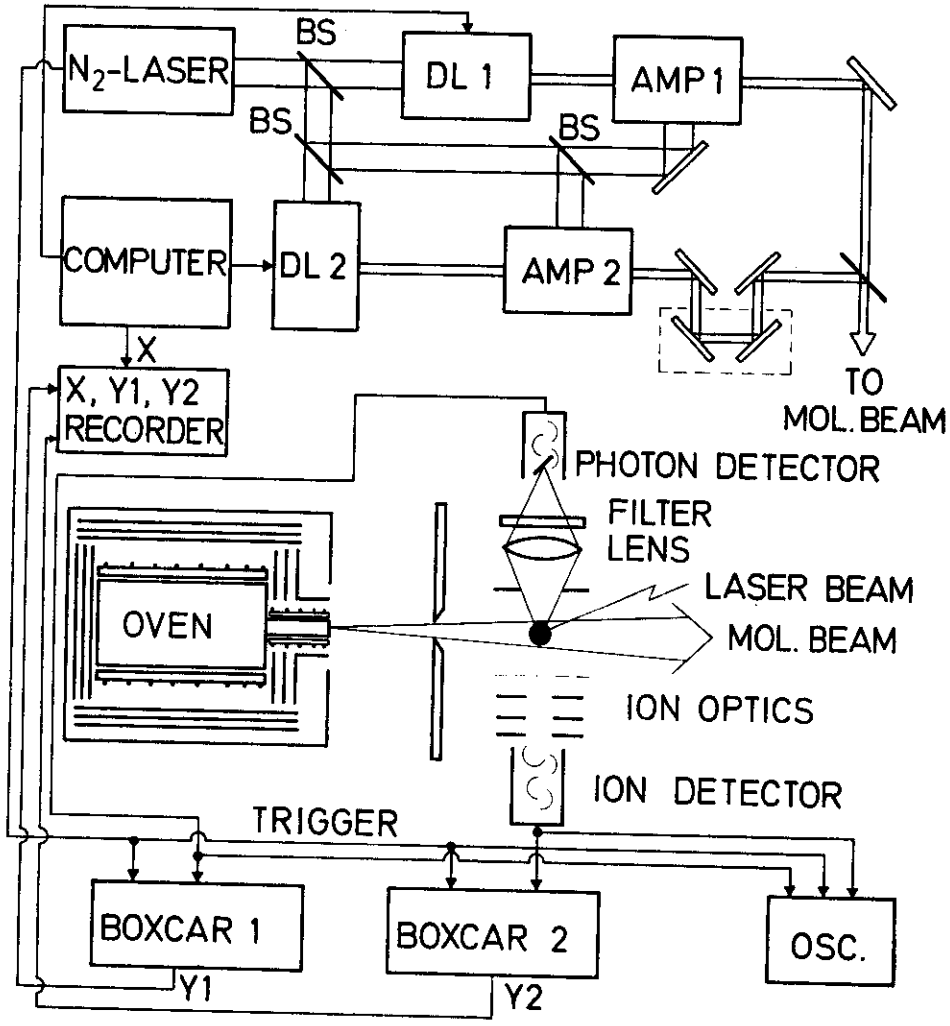
N2-LASER
BS
DL 1
AMP 1
BS
BS
COMPUTER
DL 2
AMP 2
X
X, Y1, Y2
RECORDER
TO
MOL. BEAM
PHOTON DETECTOR
FILTER
LENS
LASER BEAM
OVEN
MOL. BEAM
ION OPTICS
ION DETECTOR
TRIGGER
BOXCAR 1
BOXCAR 2
OSC.
Y1
Y2

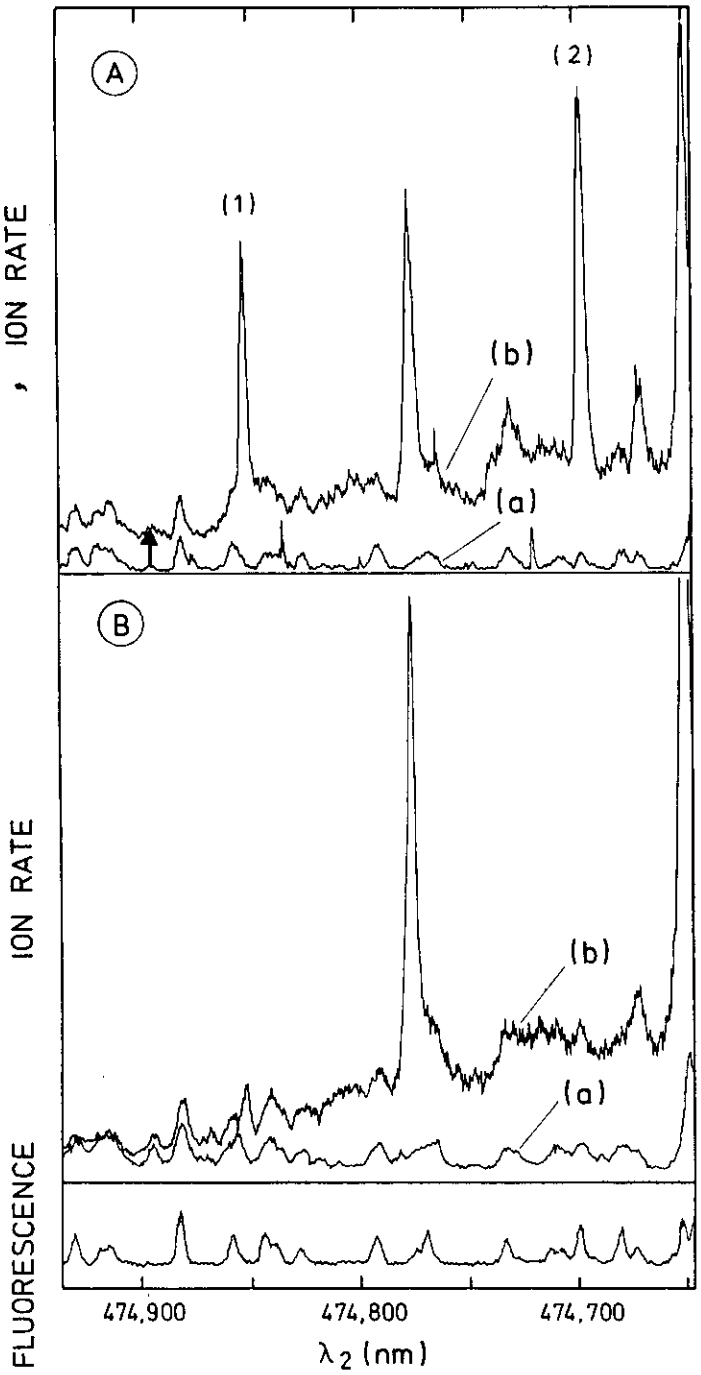
A
(1)
(2)
(b)
(a)
ION RATE
B
(b)
(a)
ION RATE
FLUORESCENCE
474,900
474,800
474,700
λ2 (nm)

Fig. 11

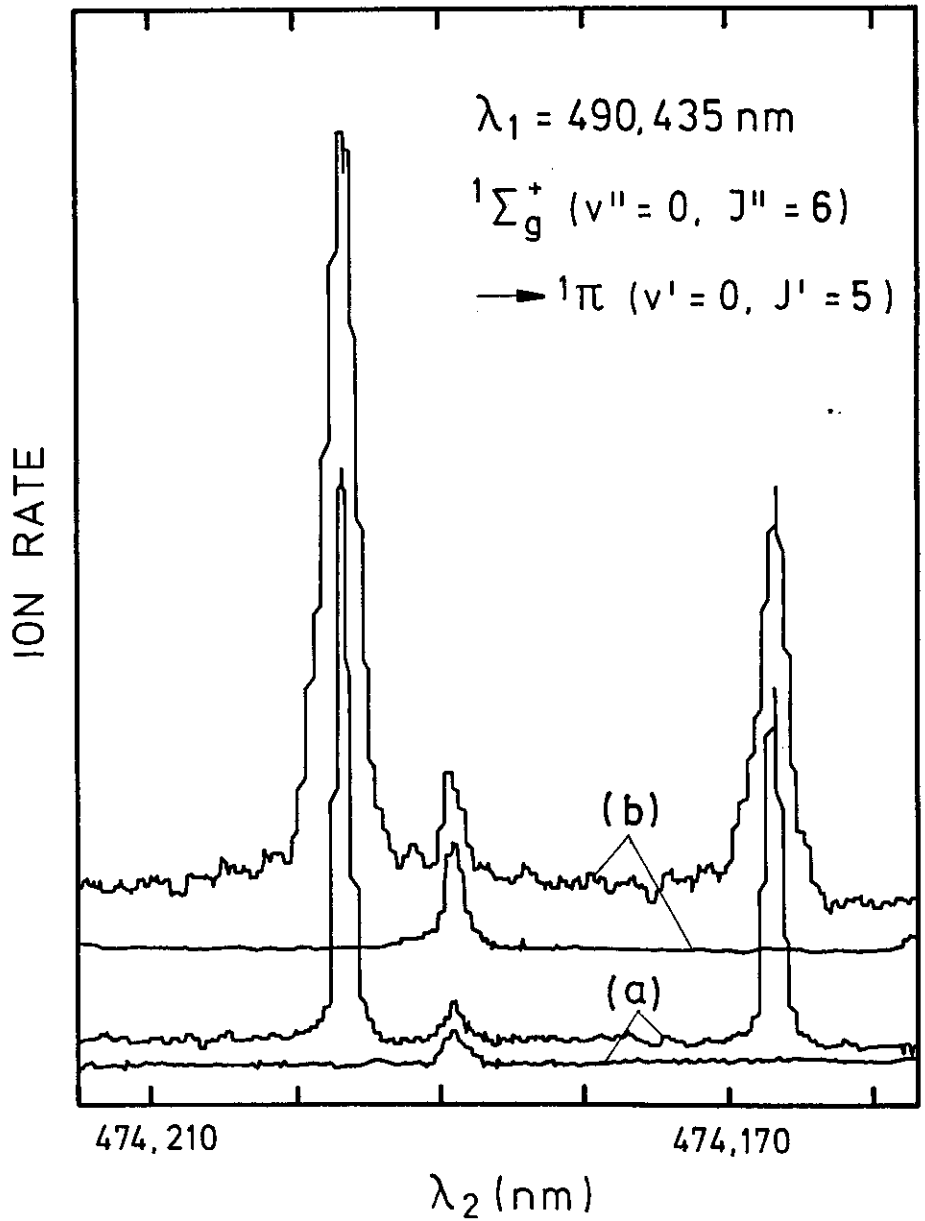
λ1 = 490,435 nm
1Σg+ (v'' = 0, J'' = 6)
→ 1π (v' = 0, J' = 5)
ION RATE
(b)
(a)
474,210
474,170
λ2 (nm)

Fig. 12

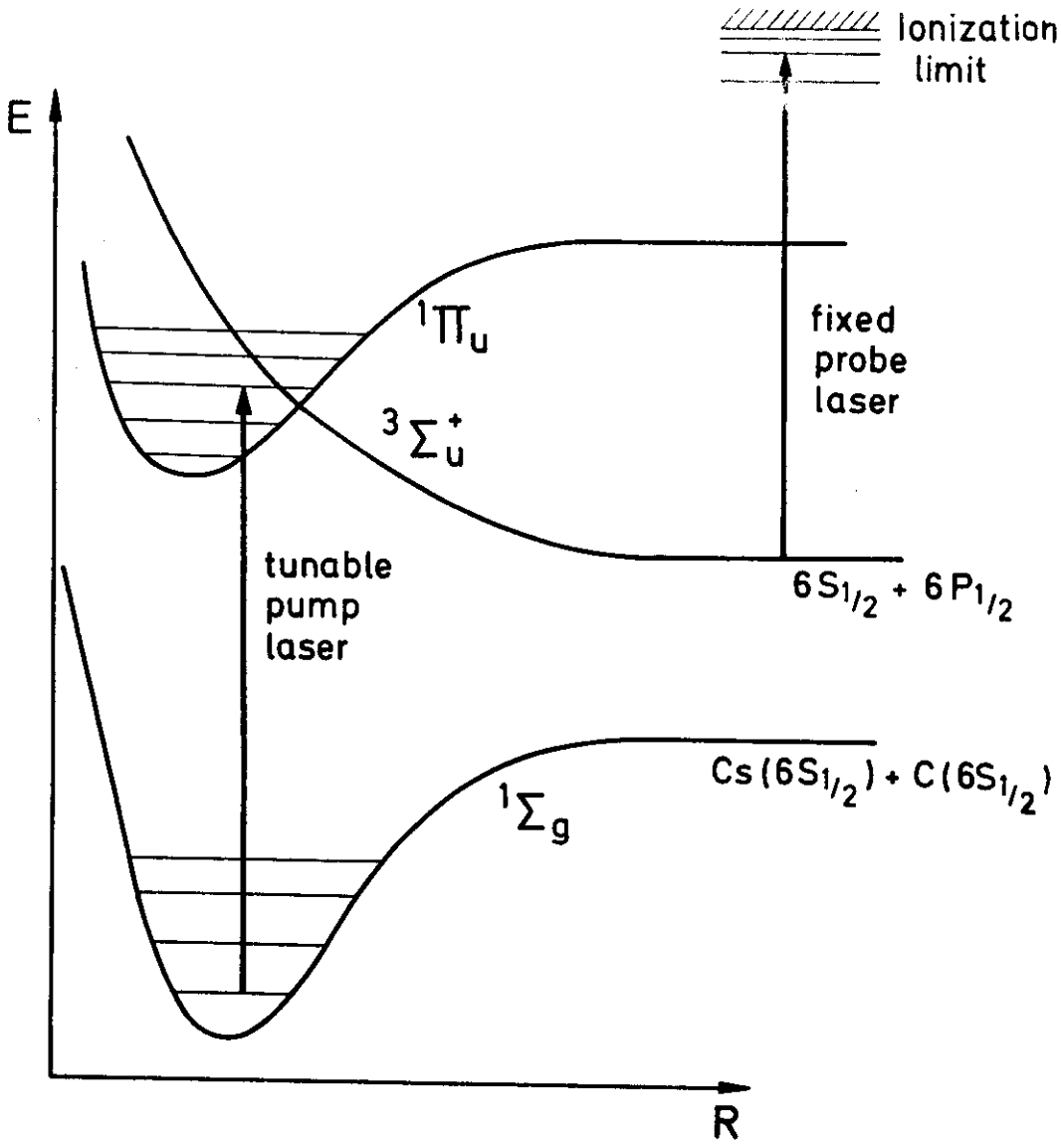
Ionization limit
E
$^1\Pi_u$
$^3\Sigma_u^+$
fixed probe laser
tunable pump laser
$6S_{1/2} + 6P_{1/2}$
$Cs(6S_{1/2}) + C(6S_{1/2})$
$^1\Sigma_g$
R

Fig. 13

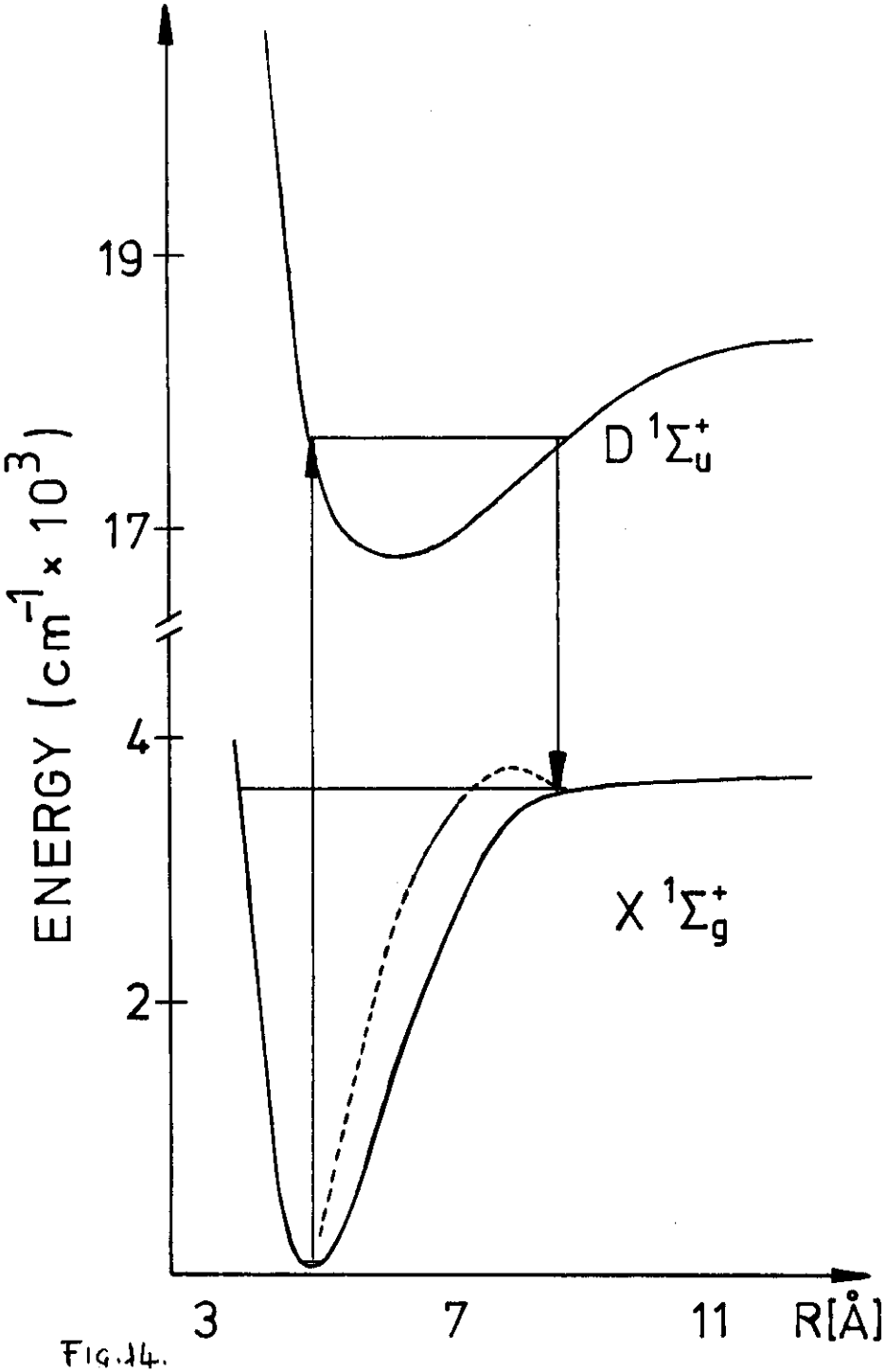
ENERGY ($cm^{-1} \times 10^3$)
19
17
4
2
$D\ ^1\Sigma_u^+$
$X\ ^1\Sigma_g^+$
3
7
11
R[Å]

Fig. 14.

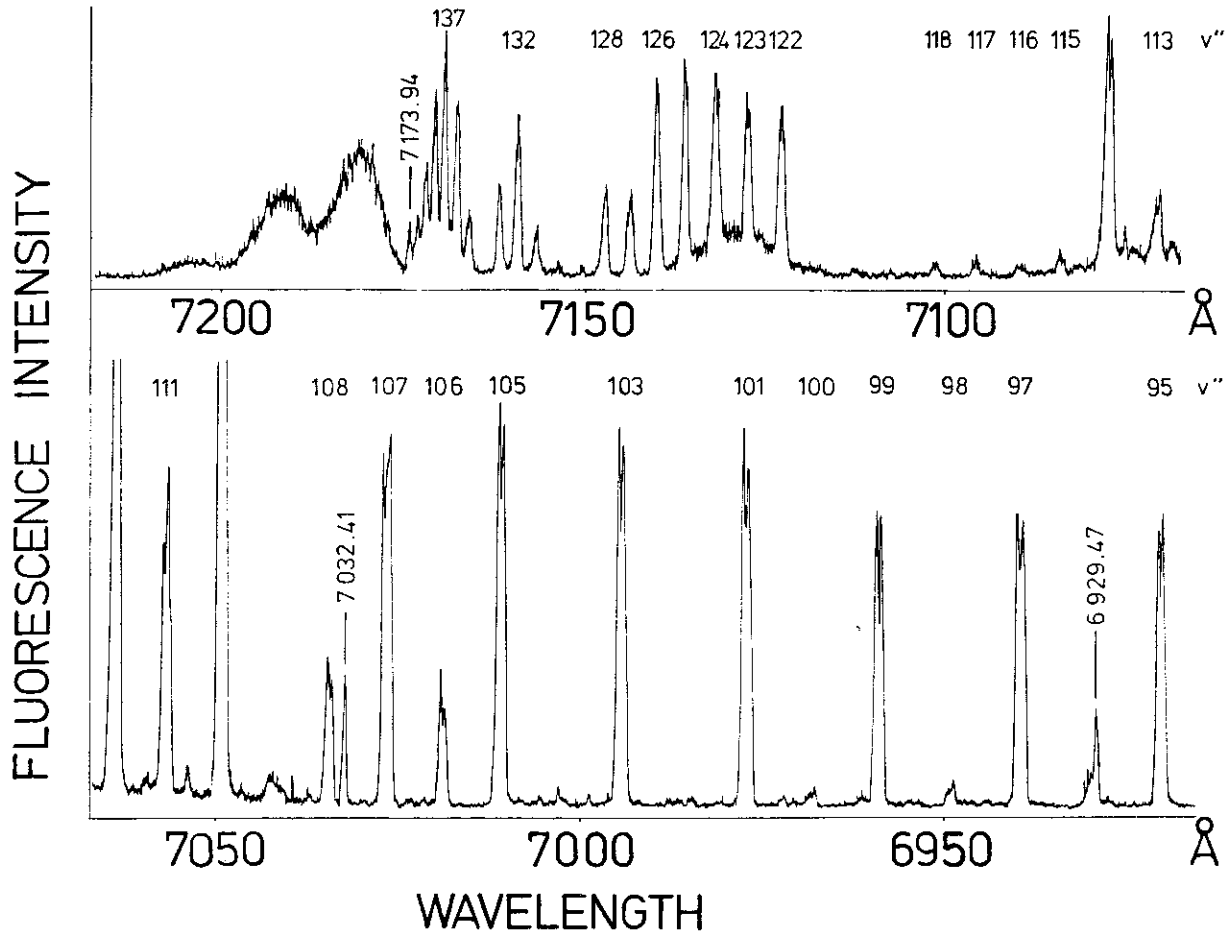
137
132
128
126
124
123
122
118
117
116
115
113
v''
7 173.94
7200
7150
7100
Å
111
108
107
106
105
103
101
100
99
98
97
95
v''
7 032.41
6 929.47
7050
7000
6950
Å
FLUORESCENCE INTENSITY
WAVELENGTH

Fig. 15

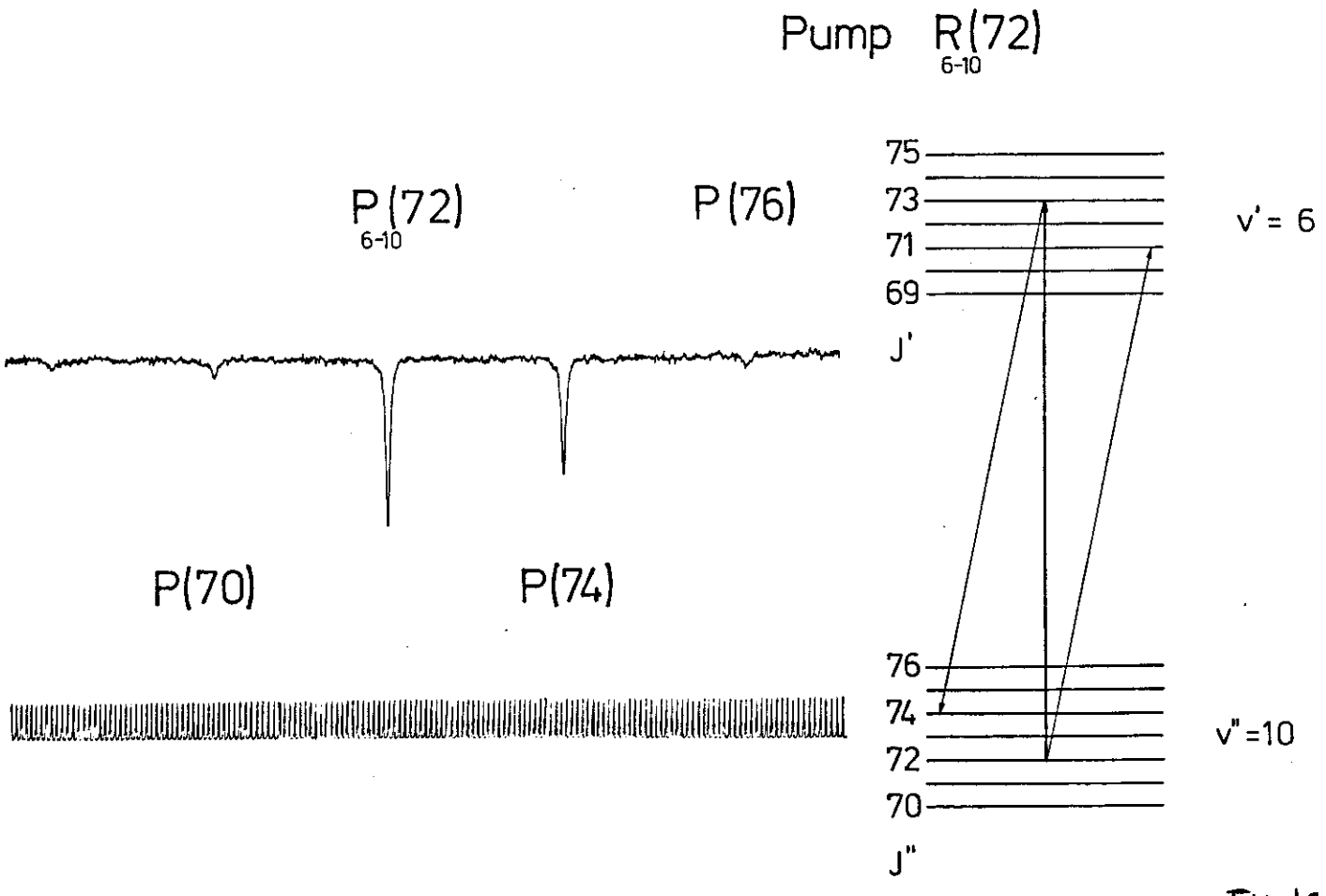
Pump R(72) 6-10
P(72) 6-10
P(76)
P(70)
P(74)
75
73
71
69
J'
v' = 6
76
74
72
70
J''
v'' = 10

Fig. 16

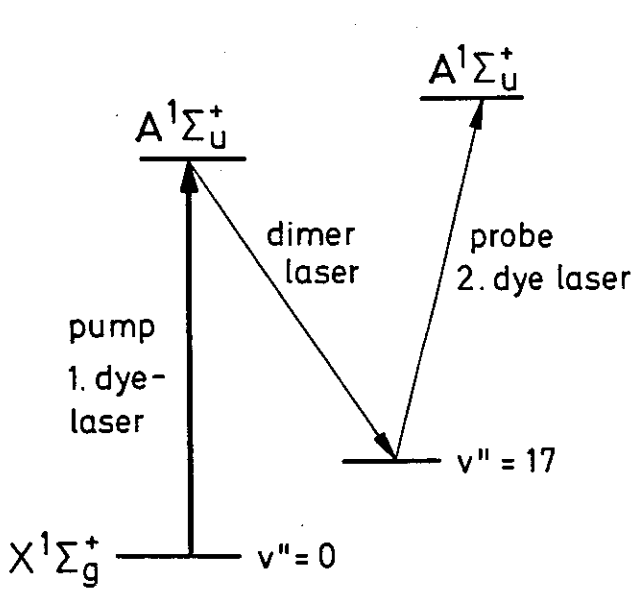
$A^1\Sigma_u^+$
$A^1\Sigma_u^+$
dimer laser
probe 2. dye laser
pump 1. dye-laser
v" = 17
$X^1\Sigma_g^+$
v"= 0

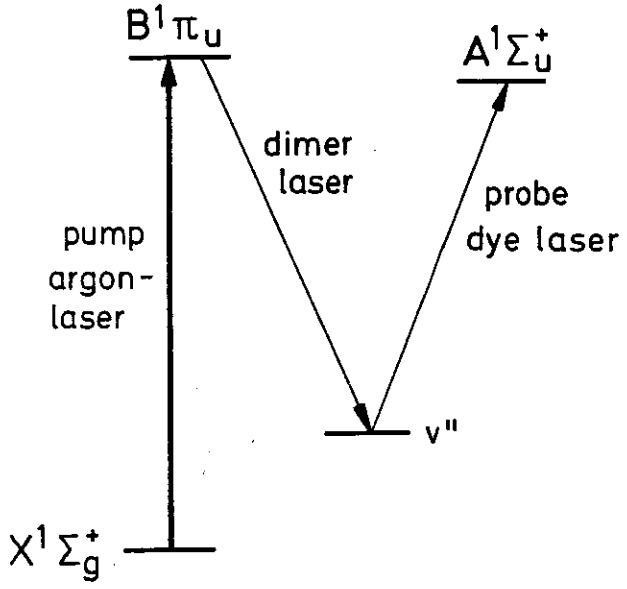
$B^1\pi_u$
$A^1\Sigma_u^+$
dimer laser
probe dye laser
pump argon-laser
v"
$X^1\Sigma_g^+$

Fig. 17

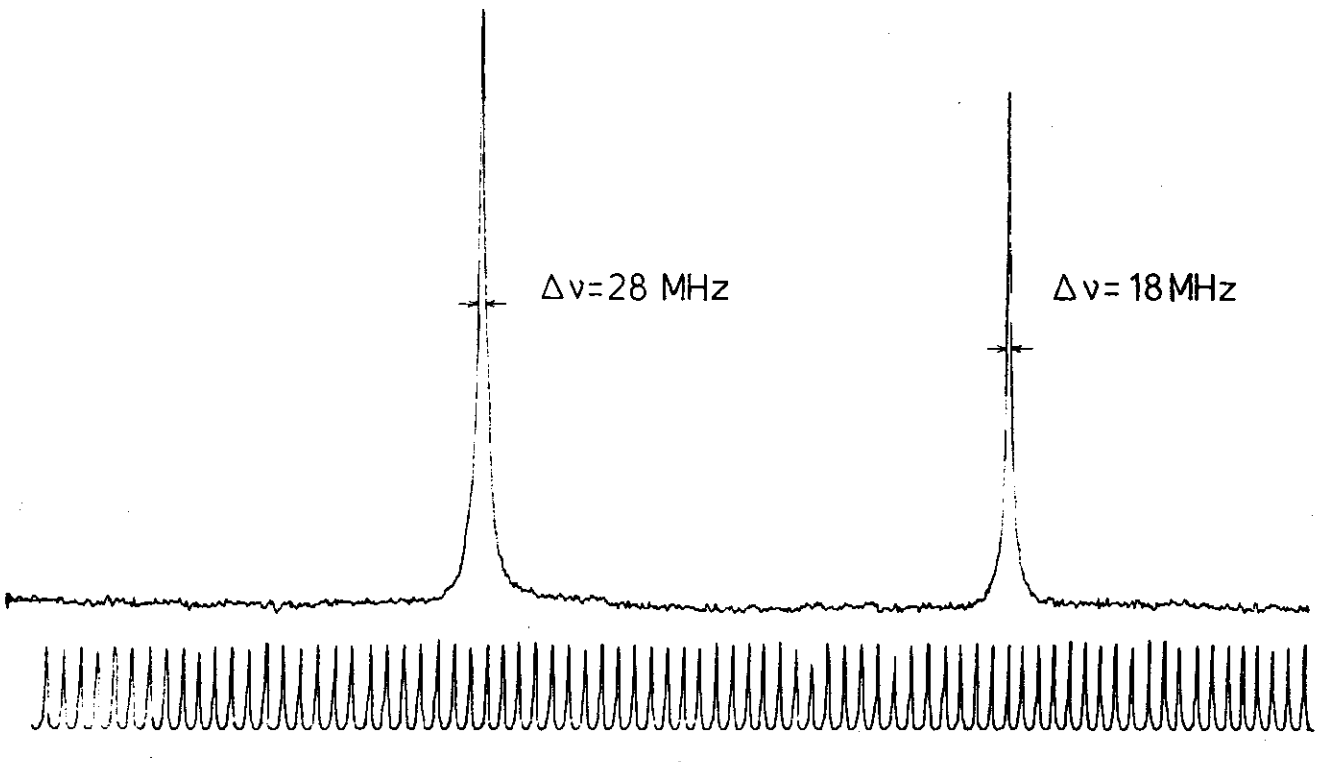
$P_{5-4}(104)$
Δν=28 MHz
Δν=18 MHz

Fig. 18